ChemComm

COMMUNICATION

View Article Online
View Journal | View Issue

Cite this: *Chem. Commun.*, 2018, **54**, 10726

Received 27th July 2018,
Accepted 17th August 2018

DOI: 10.1039/c8cc06100a

rsc.li/chemcomm

A novel mass spectrometry method based on competitive non-covalent interaction for the detection of biomarkers†

Jing Han,[ab] Yafeng Li,[a] Lingpeng Zhan,[a] Jinjuan Xue,[a] Jie Sun,[a] Caiqiao Xiong*[a] and Zongxiu Nie *[abc]

We report a novel biosensor platform based on competitive non-covalent interaction between ssDNA and a mass tag towards AuNPs, which detects PSA biomarkers sensitively, observed using MALDI MS. A detection limit of 57 pg mL^{-1} has been achieved, showing an improvement of two orders of magnitude compared to the traditional spectroscopic method.

Single-stranded DNAs (ssDNAs) are ideal biosensor probes for molecular recognition assays,[1] which can be rationally designed to detect various targets.[2,3] Among them, those conjugated with colloidal systems, like gold nanoparticles (AuNPs), are attracting increasing interest in biological applications, such as biomarker profiling.[4,5]

To prepare ssDNA–AuNP conjunction biosensors, the ssDNA is usually modified with a thiol and then attached to the AuNPs *via* sulfur–gold covalent interaction, which is a specific but expensive modified method.[6,7] A more recent method allowing the ssDNA to be adsorbed onto the colloidal surface directly is based on non-covalent interaction.[8,9] Compared with the former method, the latter has obvious advantages in terms of analytical speed, robustness and cost efficiency.

Colorimetric assay is the most commonly used detection approach in the ssDNA–AuNP non-covalent biosensors, which is easy and rapid.[10–13] Nonetheless, the development of more sensitive detection methods continues to be of great interest. For instance, in clinical diagnostics, the discrimination of early prostate cancer from benign prostatic hyperplasia partly depends on the detection sensitivity of the prostate specific antigen (PSA). A reliable method able to screen prostate diseases of varying degrees by detecting PSA sensitively would facilitate precision medical treatment.[14–18]

Herein, we report a novel MS platform based on competitive non-covalent interactions between the ssDNA and a mass tag on the AuNP surface for the detection of PSA (Scheme 1). Our method shows better sensitivity, specificity and throughput than the colorimetric assay.[19–22] In our design, the ssDNA was more non-covalently favoured by the AuNPs than the mass tag; as a result, the ssDNA occupied almost all the reaction sites on the AuNP surface, and no signal of mass tags on the AuNP surface could be detected by matrix-assisted laser desorption/ionization mass spectrometry (MALDI MS) (Scheme 1A). With the presence of biomarkers, more specific and stronger binding occurred between the biomarkers and the ssDNA, and some of the ssDNA left the surface of AuNPs and exposed free reaction sites for the mass tags. After washing and enrichment, the mass tags conjugated onto the AuNPs were detected by the MALDI MS,

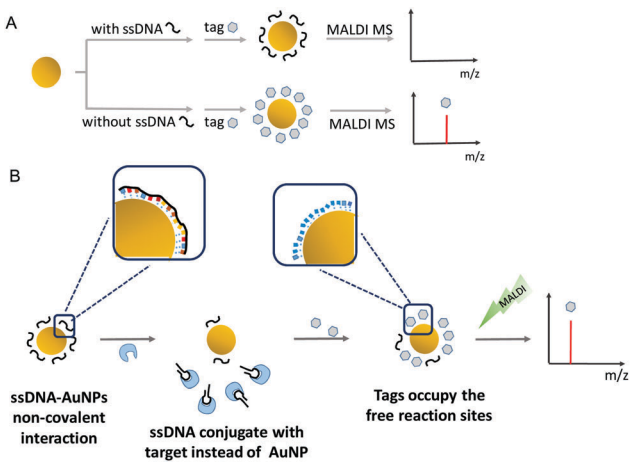

Scheme 1 Schematic view elucidating the mechanism of the whole process: (A) the competitive non-covalent interaction between ssDNA and mass tag on the AuNP surface. (B) Targeted biomarker detection through biomarker–ssDNA interaction and subsequent MALDI MS measurement of mass tags on the AuNP surface.

[a] *Beijing National Laboratory for Molecular Sciences, Key Laboratory of Analytical Chemistry for Living Biosystems, Institute of Chemistry, Chinese Academy of Sciences, Beijing, 100190, China. E-mail: xiongcq@iccas.ac.cn, znie@iccas.ac.cn*
[b] *University of the Chinese Academy of Sciences, Beijing, 100049, China*
[c] *National Center for Mass Spectrometry in Beijing, Beijing, 100190, China*

† Electronic supplementary information (ESI) available: Experimental data including synthesis and characterization of AuNPs, optimization of pH, the loading quantity, the detection limit of four bases, specificity tests, linear calibration curve and two tables. See DOI: 10.1039/c8cc06100a

and the MS signal intensity was proportional to the concentration of the biomarkers. Note that one ssDNA site could accommodate several mass tags due to their difference in molecular sizes, and the MS signal could hence be significantly amplified (Scheme 1B).

As a demonstration of our method, we employed PSA aptamers (Apt_{PSA}) as functional ssDNA to detect PSA.[23] The non-covalent interaction between AuNPs and Apt_{PSA} was initially optimized. 13 nm citrate-stabilized AuNPs were synthesized and characterized using absorption spectroscopy and transmission electron microscopy (Fig. S1–S3, ESI†). Salt concentrations affected the binding affinity between ssDNA and AuNPs due to the hydrophobic forces.[24] As shown in Fig. 1A, more Apt_{PSA} attached onto the AuNPs in the salt buffer than deionized water. The ssDNA attached onto the AuNPs with a satisfactory efficiency at pH 3, which is in accordance with previous works.[25] Other experimental conditions such as the size of AuNPs and positively charged species in solution showed minimal effects on the binding of Apt_{PSA} to the AuNPs (Fig. S5A and S6, ESI†). The prepared Apt_{PSA}–AuNP system could remain stable for 5 days (Fig. S7, ESI†).

Through varying the Apt_{PSA} concentrations added into the AuNP solution, the free Apt_{PSA} amount could be measured *via* a fluorometric method, and the loading efficiency of Apt_{PSA} was determined as the attached Apt_{PSA} ($n_{loading}$) *versus* the total amount of Apt_{PSA} (n_0) (Fig. 1B and Fig. S8, ESI†). It was found that 50 pmol Apt_{PSA} provided the best loading efficiency and was hence used in this work. The addition of PSA into the Apt_{PSA}–AuNP system could release the occupied Apt_{PSA} sites on the surface of AuNPs. The whole process could be clearly indicated using the X-ray photoelectron spectroscopy (XPS) (Fig. 1C) and UV-vis spectroscopy results (Fig. 1D). XPS measured the intensity of Apt_{PSA} on the AuNP surface. As a result, the bare AuNPs in the buffer solutions showed no XPS-detectable phosphorus (black line). Then, with Apt_{PSA} added into the AuNP solutions, the XPS P 2p signal significantly increased (red line). At last, the added PSA took away the Apt_{PSA} from the AuNPs, therefore producing a weakened (approximately 50%) XPS signal in comparison with the Apt_{PSA}–AuNP system (blue line in Fig. 1C). From the UV-vis spectroscopy results (Fig. 1D), it was found that the absorbance peak of AuNPs at 520 nm (black line) had a red shift to 650 nm (red line) with the addition of Apt_{PSA}, and moved back to 574 nm (blue line) when PSA was added into the Apt_{PSA}–AuNP system. This confirmed that this blue–red–blue shift circle clearly indicated the release of the aptamer from the gold surface. The existence of albumin and Tamm–Horsfall proteins showed little interferences to the spectroscopic and XPS data (Fig. S9, ESI†).

The XPS and UV-vis spectroscopy results show that the Apt_{PSA}–AuNPs–PSA system works nicely as proposed in Scheme 1B. Appropriate mass tags are screened to compete with Apt_{PSA}. It is reported that ssDNA conjugated with AuNPs *via* purine and pyrimidine bases. The relative affinities of bases followed the trend A > C > G > T.[26–28] Inspired by these achievements, we hypothesized that purine and pyrimidine bases as mass tags would show weaker affinity towards AuNPs than poly-bases. To confirm this suspicion, four types of bases were incubated with an Apt_{PSA}/AuNPs complex system. After two centrifugations and washing cycles, the precipitate was analyzed *via* MALDI MS. In the MALDI MS analysis, there was no signal of the mass tag without the addition of PSA (red line in Fig. 2), which means that the binding affinities of these four bases towards AuNPs are weaker than those towards Apt_{PSA}.

Next, whether these tags could serve as reporters for detecting PSA biomarkers was explored. Apt_{PSA} was first incubated with AuNPs, followed by the addition of PSA targets in the presence of the above mass tags. As shown in Fig. 2 (blue line), the addition

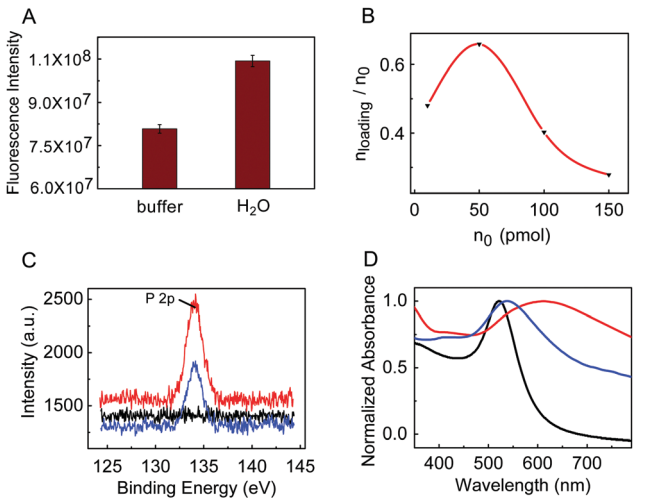

Fig. 1 (A) Fluorescence intensity of Apt_{PSA} which is not conjugated onto AuNPs in PBS buffer (pH 7.4, 10 mM) and deionized water for 24 h. The mixtures of Apt_{PSA} and AuNPs were centrifuged at a speed of 12 000 rpm for 10 min to collect the unattached Apt_{PSA} from the supernatant. (B) The Apt_{PSA} attached to the AuNPs ($n_{loading}$) at different Apt_{PSA} concentrations. The Apt_{PSA} was co-incubated with 0.52 nM AuNPs for 24 h. (C) The XPS P 2p and (D) UV-vis absorption spectra of AuNPs (black line), Apt_{PSA}–AuNPs (red line) and Apt_{PSA}–AuNPs–PSA systems (blue line).

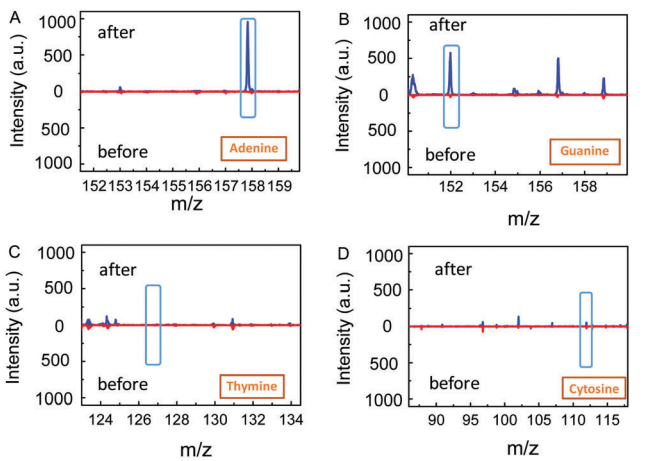

Fig. 2 Four bases were taken as the potential mass tags. The MS intensities of the potential tags, adenine (A) guanine (B) thymine (C) and cytosine (D), were measured before (red line) and after (blue line) adding the PSA target into the complexation of Apt_{PSA}/AuNPs with the mass tags.

of the PSA biomarker resulted in obvious intensities of adenine (158.0 *m*/*z*), guanine (152.0 *m*/*z*) and cytosine (112.1 *m*/*z*). Thymine (127.0 *m*/*z*) was not observed in the MS spectrum probably due to its weakest affinity to AuNPs. It is noteworthy that the peak intensity enhancement of adenine is 1000-fold, which is larger than those of the others. The MS intensity followed the trend of A > G > C > T, which may result from the influence of binding affinity and desorption and ionization efficiency. Considering the stronger binding affinity and MS signal resolution, adenine would be employed for the following examination. All the experiments were replicated on five different days, which showed a good repeatability (Fig. S10, ESI†). In addition, the size of AuNPs is optimized, and 13 nm AuNPs with excellent performance and easy synthesis were chosen in the following experiments (Fig. S5B, ESI†).

To test the selectivity of our method, control experiments with the addition of other proteins such as human serum albumin (HSA), immunoglobulin G (IgG), transferrin (TF), fetal bovine serum (FBA) and a mixture of FBA and PSA were performed. The Tamm–Horsfall protein as the most abundant protein in urine was also used with two concentrations (1 and 10 mg mL^{-1}). As shown in Fig. S11 (ESI†), the non-covalent interaction between Apt_{PSA} and AuNPs could not be broken by adding the nonspecific proteins, implying the high specificity of our method for PSA detection.

Having demonstrated the ability of adenine as the potential mass tag and the specificity of our general biosensor, next we studied whether the competitive non-covalent biosensor could distinguish the subtle change of the PSA level. As shown in previous studies,[14,15] a reliable method able to analyze various levels of PSA can lead to the development of screening methods of prostate diseases of varying degrees and thus providing a better performance of precision medical treatment. For this purpose, different concentrations of PSA biomarker were detected using Apt_{PSA}/AuNPs with adenine tags. As shown in Fig. 3, with increasing the concentrations of PSA biomarker from 0 to 6 ng mL^{-1}, the intensity of the adenine peak showed a significant difference (Fig. 3A). In comparison, the traditional colorimetric assays could not distinguish subtle changes of PSA below 0.6 ng mL^{-1} (Fig. 3C). As shown in Fig. 3B and D, the intensity of the MS signal increased by 91-fold but the ratio of A_{650}/A_{520} only increased by 2.5-fold when the concentration of PSA was up to 6 ng mL^{-1}. The colorimetric assays rely on the detection of AuNP aggregation and their poor performance may be attributable to the low aggregation efficiency of AuNPs below 0.6 ng mL^{-1}.

To improve the reproducibility, an internal standard (IS) 3-methyladenine was introduced in the MALDI-TOF MS analysis (Fig. S12, ESI†). The detection limit is 57 pg mL^{-1} according to the 3σ rule[29–31] (defined as DL = 3*S*/*m*, where *m* is the slope of the corresponding calibration curve and *S* is the standard deviation of the blank) in our approach (Fig. S13 and Table S1, ESI†), which is improved two orders of magnitude compared with the traditional colorimetric assays with a detection limit estimated to be 1.18 ng mL^{-1} (Fig. S14 and Table S2, ESI†) and the enzyme linked immunosorbent assay (ELISA) with a detection

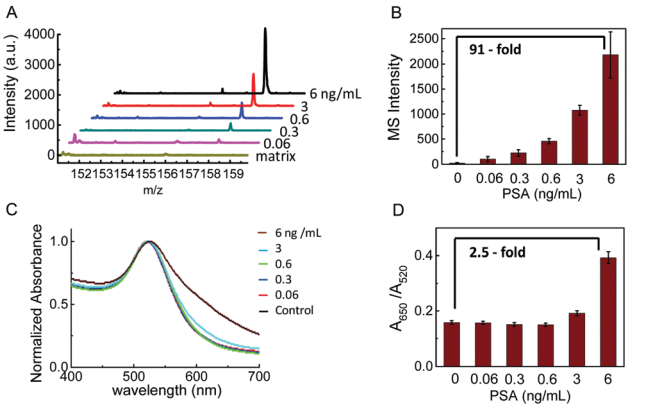

Fig. 3 (A) MALDI-TOF MS spectral signals of adenine as the mass tag are distinguishable in the presence of PSA with various concentrations (0.06, 0.3, 0.6, 3 and 6 ng mL^{-1}), and the MS signals of the matrix (CCA) are clean in the range of 150–160 *m*/*z*. (B) The intensity changes of the mass tag in the presence of PSA with various concentrations (0, 0.06, 0.3, 0.6, 3 and 6 ng mL^{-1}). (C) In traditional colorimetric assays, Apt_{PSA}–PSA target interaction induces the aggregation of AuNPs, and the absorbance changes of AuNPs with the addition of aptamer (1 μM, 100 μL), NaCl (10 μL, 30 mM) and PSA with various concentrations (0.06, 0.3, 0.6, 3 and 6 ng mL^{-1}) are given. The absorbance did not change significantly with the concentration of PSA below 0.6 ng mL^{-1}. The absorption at 520 nm was normalized to 1.0. (D) A_{650}/A_{520} reflects the intensity of AuNP aggregation with various concentrations of PSA (0.06, 0.3, 0.6, 3 and 6 ng mL^{-1}). AuNPs would not aggregate when the concentration of PSA is below 0.6 ng mL^{-1}.

limit of 2.32 ng mL^{-1} (Fig. S15 and Table S3, ESI†). Compared to other approaches, our competitive non-covalent platform showed a notable advantage of sensitivity in the low concentration range (Table S4, ESI†).

Next, a recovery experiment was carried out by adding different numbers of PSA protein into healthy human urine, and the fluctuation of the salt in urine did not affect the assays (Fig. S16, ESI†). As shown in Fig. S17 and Table S5 (ESI†), this method has a robust resistibility to the complex biological matrix with a satisfactory recovery ranging from 88.37% to 108.88%. These results clearly indicated that the novel method can be applied to detect trace amount of PSA in human urine with good accuracy.

To demonstrate the potential of the developed method for clinical sample assays, our method was applied for the detection of PSA in urine samples and compared it to ELISA. The results showed that the concentrations of PSA protein determined using our method were almost consistent with those determined using ELISA (Table S6, ESI†). In addition, our approach could also detect the PSA that spiked into serum (Fig. S18, ESI†). These data revealed the potential of the developed method for PSA detection in point-of-care clinical applications.

In summary, we have demonstrated a novel sensor platform based on competitive non-covalent interaction between ssDNA and a competitive mass tag towards AuNPs to capture and profile biomarkers in a high-throughput and sensitive manner. This biosensor takes advantage of the nature of aptamers as recognition moieties and conjugated onto AuNPs *via* non-covalent interaction. We showed that this novel approach could

clearly detect the subtle changes of the cancer marker level in the complex with a lower detection limit compared with traditional colorimetric assays, making this strategy applicable to the analysis of clinical specimens. Moreover, such an integrated approach may serve as a model for many other biomarker detection systems to boost the development of biosensors.

This study was supported by grants from the National Natural Science Foundation of China (Grant No. 21625504, 21827807, 21475139, 21505140, 21621062 and 21790390/21790392) and Chinese Academy of Sciences.

Conflicts of interest

There are no conflicts to declare.

Notes and references

1 A. P. Turner, *Chem. Soc. Rev.*, 2013, **42**, 3184–3196.
2 S. Song, L. Wang, J. Li, C. Fan and J. Zhao, *TrAC, Trends Anal. Chem.*, 2008, **27**, 108–117.
3 M. Gao, D. Daniel, H. Zou, S. Jiang, S. Lin, C. Huang, S. M. Hecht and S. Chen, *Chem. Commun.*, 2018, **54**, 968–971.
4 C. Li, T. Chen, I. Ocsoy, G. Zhu, E. Yasun, M. You, C. Wu, J. Zheng, E. Song, C. Huang and W. Tan, *Adv. Funct. Mater.*, 2014, **24**, 1772–1780.
5 Y. Chen, S. C. Kung, D. K. Taggart, A. R. Halpern, R. M. Penner and R. M. Corn, *Anal. Chem.*, 2010, **82**, 3365–3370.
6 D. Liu, A. Bruckbauer, C. Abell, S. Balasubramanian, D. Kang, D. Klenerman and D. Zhou, *J. Am. Chem. Soc.*, 2006, **128**, 2067–2071.
7 D. Y. Petrovykh, H. Kimura-Suda, L. J. Whitman and M. J. Tarlov, *J. Am. Chem. Soc.*, 2003, **125**, 5219–5226.
8 A. Opdahl, D. Y. Petrovykh, H. Kimura-Suda, M. J. Tarlov and L. J. Whitman, *Proc. Natl. Acad. Sci. U. S. A.*, 2007, **104**, 9–14.
9 S. Wang, X. Cai, L. Wang, J. Li, Q. Li, X. Zuo, J. Shi, Q. Huang and C. Fan, *Chem. Sci.*, 2016, **7**, 2722–2727.
10 Y. Jiang, M. Shi, Y. Liu, S. Wan, C. Cui, L. Zhang and W. Tan, *Angew. Chem., Int. Ed.*, 2017, **56**, 11916–11920.
11 H. Li and L. Rothberg, *Proc. Natl. Acad. Sci. U. S. A.*, 2004, **101**, 14036–14039.
12 W. Zhao, W. Chiuman, J. C. F. Lam, M. A. Brook and Y. Li, *Chem. Commun.*, 2007, 3729–3731.
13 Y. Huo, L. Qi, X. J. Lv, T. Lai, J. Zhang and Z. Q. Zhang, *Biosens. Bioelectron.*, 2016, **78**, 315–320.
14 R. Etzioni, N. Urban, S. Ramsey, M. McIntosh, S. Schwartz, B. Reid, J. Radich, G. Anderson and L. Hartwell, *Nat. Rev. Cancer*, 2003, **3**, 243–252.
15 K. S. Kerian, A. K. Jarmusch, V. Pirro, M. O. Koch, T. A. Masterson, L. Cheng and R. G. Cooks, *Analyst*, 2015, **140**, 1090–1098.
16 Y. Lin, Y. L. Ying, X. Shi, S. C. Liu and Y. T. Long, *Chem. Commun.*, 2017, **53**, 11564–11567.
17 R. J. Yu, W. Ma, X. Y. Liu, H. Y. Jin, H. X. Han, H. Y. Wang, H. Tian and Y. T. Long, *Theranostics*, 2016, **6**, 1732–1739.
18 X. Y. Long, Z. J. Zhang, J. Y. Li, D. Shenga and H. Z. Lian, *Chem. Commun.*, 2017, **53**, 4620–4623.
19 A. K. Yocum, A. P. Khan, R. Zhao and A. M. Chinnaiyan, *Proteomics*, 2010, **10**, 3506–3514.
20 Z. He, Q. Chen, F. Chen, J. Zhang, H. Li and J. M. Lin, *Chem. Sci.*, 2016, **7**, 5448–5452.
21 J. L. Zhang, Z. Li, C. S. Zhang, B. S. Feng, Z. G. Zhou, Y. Bai and H. W. Liu, *Anal. Chem.*, 2012, **84**, 3296–3301.
22 L. Qiao, C. Roussel, J. Wan, J. Kong, P. Yang, H. H. Girault and B. Liu, *Angew. Chem., Int. Ed.*, 2008, **47**, 2646–2648.
23 V. K. Tamboli, N. Bhalla, P. Jolly, C. R. Bowen, J. T. Taylor, J. L. Bowen, C. J. Allender and P. Estrela, *Anal. Chem.*, 2016, **88**, 11486–11490.
24 T. M. Herne and M. J. Tarlov, *J. Am. Chem. Soc.*, 1997, **119**, 8916–8920.
25 X. Zhang, M. R. Servos and J. Liu, *J. Am. Chem. Soc.*, 2012, **134**, 7266–7269.
26 A. Gourishankar, S. Shukla, K. N. Ganesh and M. Sastry, *J. Am. Chem. Soc.*, 2004, **126**, 13186–13187.
27 L. M. Demers, M. Östblom, H. Zhang, N. H. Jang, B. Liedberg and C. A. Mirkin, *J. Am. Chem. Soc.*, 2002, **124**, 11248–11249.
28 M. Östblom and B. Liedberg, *J. Phys. Chem. B*, 2005, **109**, 15150–15160.
29 A. E. Radi, J. L. A. Sánchez, E. Baldrich and C. K. O'Sullivan, *J. Am. Chem. Soc.*, 2006, **128**, 117–124.
30 R. Akter, M. A. Rahman and C. K. Rhee, *Anal. Chem.*, 2012, **84**, 6407–6415.
31 R. P. Buck and E. Lindner, *Pure Appl. Chem.*, 1994, **66**, 2527–2536.